Geometric Accuracy Assessment of Unmanned Digital Cameras and LiDAR Payloads

Mohamed M. R. Mostafa, Stefanie Van-Wierts, and Vi Huynh

Microdrones, 2911 Rue Du Meunier, Vaudreuil-Dorion, J7V 8P2 Quebec, Canada – mohamed.mostafa@microdrones.com

Abstract

Over the last few years, a number of sophisticated multi-sensor systems have been integrated onboard Unmanned Aerial platforms. This allows for producing a variety of mapping products for different mapping applications. Recently, the resulting final mapping product accuracies match those of the traditional well-engineered manned systems. This paper presents the results of development and testing of a fully integrated unmanned systems for professional grade mapping. There are a number of parameters that either individually or collectively affect the quality and accuracy of a final airborne mapping product. This paper focuses on identifying the attainable accuracy when using a metric camera or a LiDAR payload onboard a drone. Assessment of the final ground object positioning accuracy is presented through real-world test flight missions flown in Canada and the USA.

1. Introduction

A Geometric accuracy assessment is presented in this paper for two Microdrones systems; namely: mdMapper1000DG and mdLiDAR1000 as shown in Figure 1 and Figure 2, respectively. A number of test flights and flight missions are used for this illustrating the results of the geometric accuracy assessment exercise presented in this paper.

Figure 1: Microdrones mdMapper1000DG

Figure 2: Microdrones mdLiDAR1000

2. Accuracy Assessment of The mdMapper1000DG System

Eight flights were flown using Microdrones mdMapper1000DG equipped with Sony RX1RII camera integrated with Trimble APX-15 as shown in Figure 1. The flights took place in Montreal, Canada on September 20th, 2016. Multiple flight heights were flown in order to examine the different Ground Sample Distance (GSD) effect on geometric accuracy. All flights have been flown at an 80x80 overlap/sidelap. They were reduced to 80x60, 80x40, and 60x40 at the processing stage in order to examine the effect of overlap/sidelap on geometric accuracy.

A new dedicated base station was accurately established 900 m away from the centre of the Area of Interest (AOI) as shown in Figure 3. Additionally, 2 Cansel CORS stations where used for accuracy and Quality Control Purposes, as shown in Figure 4. Furthermore, the Canadian Spatial Reference System (CSRS) online processing tool was used.

The new base station was used to establish 14 Ground Control Points (GCP's) as well as being used as the main base station for all the flights. This guaranteed that all the positional components of the entire test flights including trajectory and GCP's are referenced to the same base station. All GCP's have been accurately established and signalized using geodetic GNSS receivers coupled with Geodetic antennas for multipath mitigation and proper noise and antenna phase centre handling. The GNSS data acquisition technique was designed in order to achieve the best possible positioning accuracy of the GCP's. A total of 891 data processing configurations were used in order to identify the overall system performance.

Figure 3 Base Station location near the Area of Interest (AOI)

Figure 4: Base Station Location Relative to Cansel GNSS Stations

2.1 The Base station

The base station is a critical component for accuracy assessment. Therefore, the following configuration has been devised in order to achieve the project goals, including:

- The base station is used for both flights and for establishing GCP's
- The base station must have a geodetic accuracy in an absolute sense that is equivalent or higher than the highest resolution of the data acquired in this project
- The base station coordinates must be computed independently from multiple sources in an absolute sense in order to confirm the validity of the final base station positioning accuracy.

The Base station data acquisition has been done using Trimble BD930 GNSS receiver equipped with a Zephyr II Geodetic antenna for multipath mitigation purposes. The Base station data has been collected over the course of 2 Sessions as shown in Table 1. Two Cansel permanent tracking GNSS Network Stations have been used in this project, namely: SHER and DRUM. Table 1 lists their data acquisition time durations while Figure 4 shows their location relative to the AOI.

The aforementioned Base Station data has been processed 8 different times using different configuration. The Average coordinates of the eight processing results was used as a reference. The statistics of the residuals for the eight solutions compared to the reference are listed in Table 3.

Table 1: Base Station Date Acquisition Sessions

ID	Session	Date		GPS Local Time		Duration
		Start	End	Start	End	hh:mm:ss
Base Station	1	19-Aug	20-Aug	22:12:13	11:01:38	12:49:25
Base Station	2	20-Aug	20-Aug	11:02:08	22:30:36	11:28:28

Table 2: SHER & DRUM Data Acquisition Timing

ID	Session	Duration	Comments
		[hh:mm:ss]	
SHER	1	14:59:59	Overnight data
SHER	2	13:59:59	+ 1 day (Total duration: > 36hrs)
DRUM	1	14:59:59	Overnight data
DRUM	2	13:59:59	+ 1 day (Total duration: > 36hrs)

Table 3: Base Station Statistics

Stats	dE (m)	dN (m)	dH (m)
Min	-0.001	-0.005	-0.007
Max	0.003	0.002	0.006
Mean	0.001	-0.001	-0.002
Σ	0.001	0.003	0.005
RMS	0.002	0.003	0.006

2.2 Ground Control and Check Points

The Ground Control Point (GCP) and Check point layout, distribution and observation configuration have been designed in order to satisfy a number of conditions, including GCP coverage for different testing scenarios including different image strips, blocks, etc. and the highest possible absolute positioning accuracy. A total of fourteen (14) Ground Control Points (GCP's) were established in the DOMTAR test flight area as shown in Figure 5. All GCPs were painted on the ground as shown in Figure 6. The data acquisition configuration was devised to collect data in a static mode at each GCP. The project base station was simultaneously and continuously collecting GNSS data during the entire GCP data acquisition time.

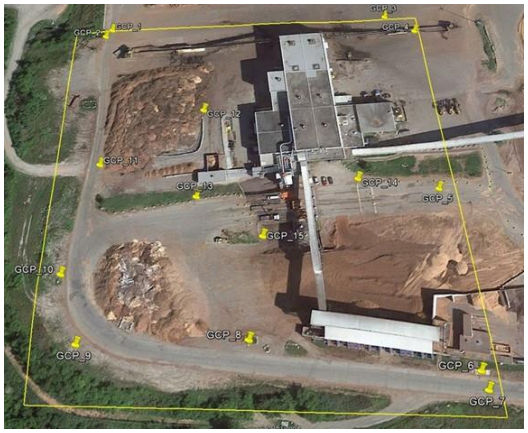

Figure 5: Ground Control Point Layout

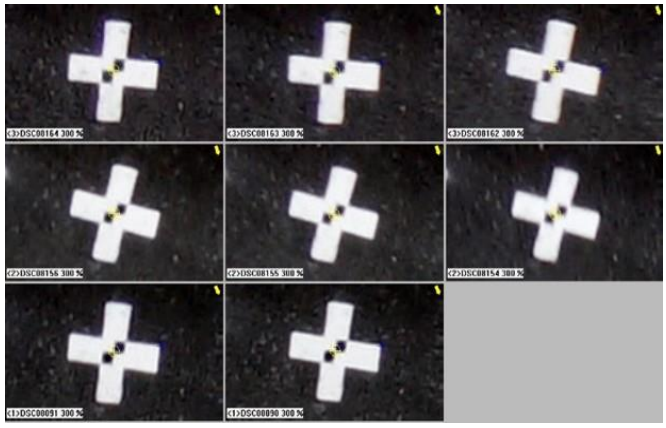

Figure 6: Ground Control displayed on Imagery

Table 4: GCP Statistics

ID	RMS Easting [m]	RMS Northing [m]	RMS Height [m]
GCP01	0.007	0.009	0.018
GCP02	0.007	0.008	0.013
GCP03	0.006	0.011	0.017
GCP04	0.006	0.009	0.017
GCP05	0.006	0.010	0.016
GCP06	0.007	0.009	0.012
GCP07	0.006	0.009	0.012
GCP08	0.005	0.007	0.014
GCP09	0.007	0.009	0.013
GCP10	0.006	0.009	0.017
GCP11	0.007	0.015	0.018
GCP12	0.006	0.009	0.014
GCP13	0.006	0.009	0.012
GCP14	0.011	0.020	0.032

2.3 Accuracy Assessment Results

This Section is dedicated to briefly demonstrate the accuracy assessment results using different flights flown in this project. Each flight contained an average of twenty image strips and 30 images per strip to cover the entire Area of Interest at a certain flight altitude. In order to produce multiple image blocks and multiple overlap/sidelap combinations, the following was carried out**:**

- A number of 4-strip blocks have been extracted from the data
- Different levels of overlap and sidelap have been extracted from the data

This resulted in a variety of 4-strip blocks with different levels of overlap and sidelap at two different flight altitudes; namely 60m and 120 m, respectively. Some flights have been flown using Microdrones new gravity-based Nadir mount that is designed to allow for roll and pitch real time compensation while other flights have been flown using a fixed mount. The effect of these two mounts is also analysed. Further, two cameras have been flown namely, Sony a7R and Sony Rx1RII. The latter has better weight, power consumption and ground coverage. The effect of the two cameras on the results is also analysed. Camera lab calibration versus airborne calibration is also analysed.

Figure 7 shows the RMS of Check Point Residuals for flight # 2 flown at 60 m Above Ground Level (AGL) which when coupled with the RX1RII 35 mm focal length resulted in a Ground Sample Distance (GSD) of 8 mm. Seven 4-strip blocks are shown in Figure 7 extracted from flight # 2 at 80x80 endlap/sidelap. Figure 8 shows the same results at 80x40 endlap/sidelap.

Figure 9 and Figure 10 show the RMS of Check Point Residuals for 3-strip blocks at 80x80 and 80x40 endlap/sidelap. Figure 11 and Figure 12 show the RMS of Check Point Residuals for 2-strip blocks at 80x80 and 80x40 endlap/sidelap.

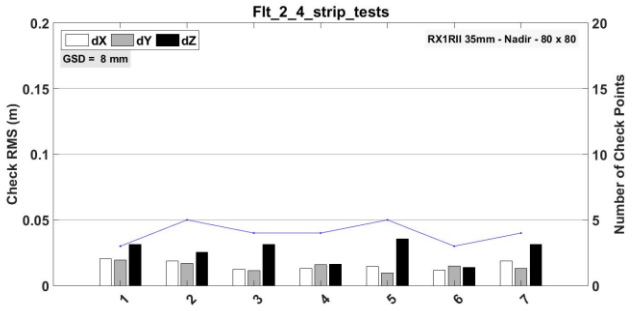

Figure 7: RMS of Check Point Residuals - Flight # 2 - four image strips - 80x80 overlap - GSD = 8 mm

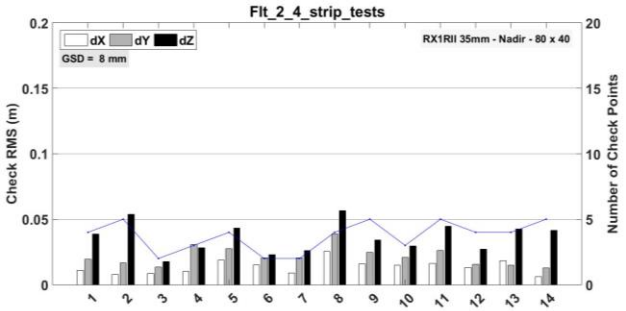

Figure 8: RMS of Check Point Residuals - Flight # 2 - four image strips - 80x40 overlap - GSD = 8 mm

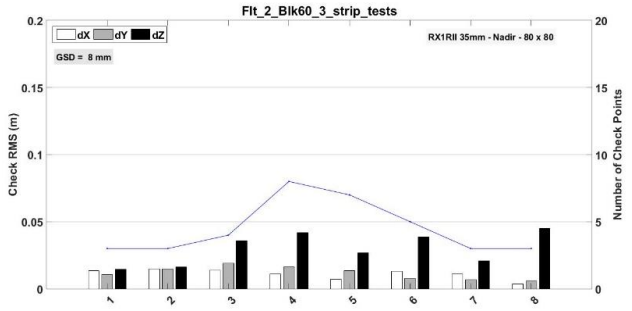

Figure 9: RMS of Check Point Residuals - Flight # 2 - Three image strips - 80x80 overlap - GSD = 8 mm

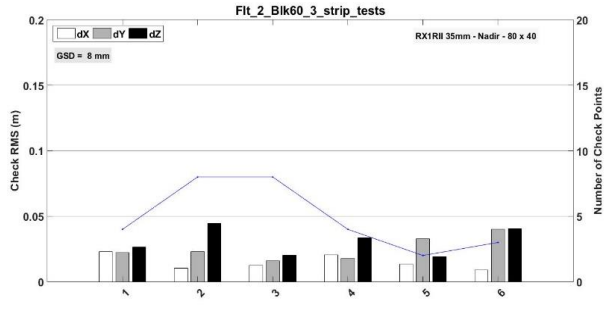

Figure 10: RMS of Check Point Residuals - Flight # 2 - Three image strips - 80x40 overlap - GSD = 8 mm

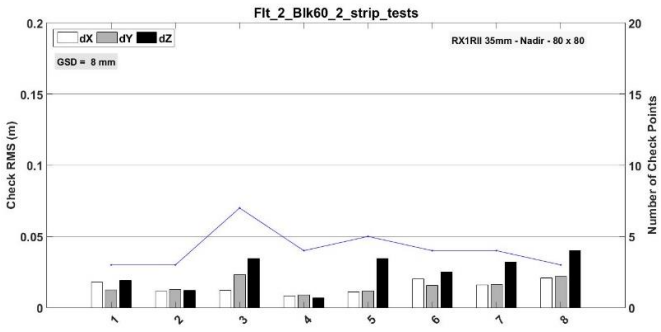

Figure 11: RMS of Check Point Residuals - Flight # 2 - Two image strips - 80x40 overlap - GSD = 8 mm

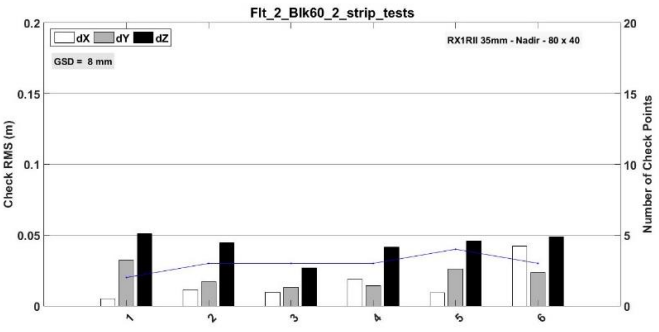

Figure 12: RMS of Check Point Residuals - Flight # 2 - Two image strips - 80x40 overlap - GSD = 8 mm

3. Accuracy Assessment of The mdMapperLiDAR1000 System

The mdLiDAR1000 is a fully integrated Unmanned LiDAR system that includes a Sick LiDAR integrated with a Trimble APX15 direct georeferencing system. The Technical specifications of mdLiDAR1000 are listed in Table 5.

Table 5: mdLiDAR1000 Technical Specifications

Flight Altitude AGL* (m/ft)	30/100	40/130	50/165
Speed (m/s)	Point Density (pts/m²)**		
2	160	120	95
3	105	80	65
4	80	60	50
5	65	50	40
Swath width (m)	55	75	95
Flight time (minutes)***	25	25	25
Number of Laser Returns	3	3	3
Area cover at 20% overlap (hectare)****	19	30	38
Area cover at 50% overlap (hectare)****	15	19	24

*Flight Altitude Above Ground Level (AGL)
**Average Point density. Note that calculation does not factor target remission (reflectivity) %
***Flight time is calculated under standard flight conditions (using new Microdrones batteries)
****Area Coverage for a survey of 20 minutes at a flight speed of 5m/s

In order to adequately assess the final absolute positioning accuracy of the 3D LiDAR point cloud, a number of test flights have been conducted at the Griffiss airport in New York. A dense network of GCP's covered a segment of the entire runway and taxiway at Griffiss airport. The GCP's were established in a similar manner of those GCPs discussed above. The total number of GCP's on the runway are 56 and 18 on the taxiway as shown in Figure 13 and Figure 14 while Table 6 lists the flights done using mdLiDAR1000 for accuracy assessment purposes.

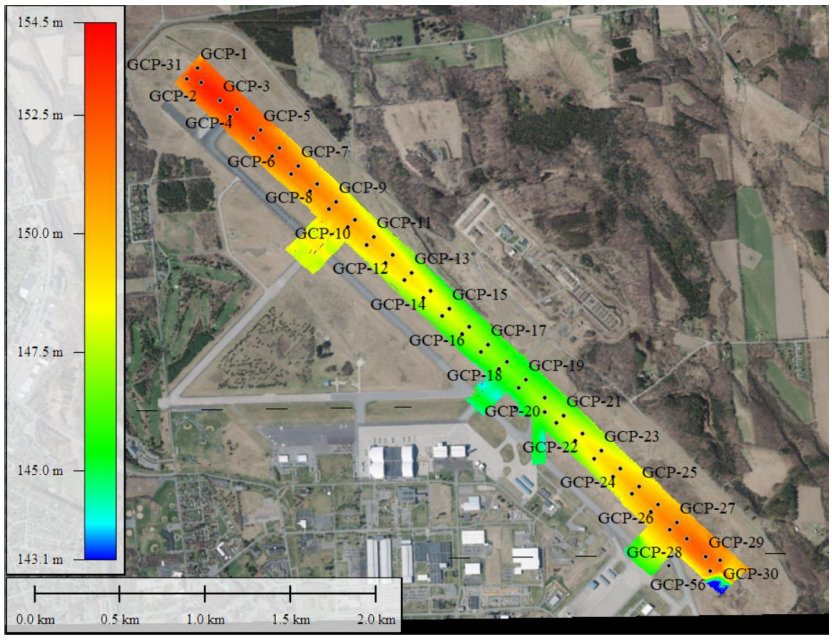

Figure 13: Figure 13: Ground Control Point Distribution at the Griffiss Airport Runway.

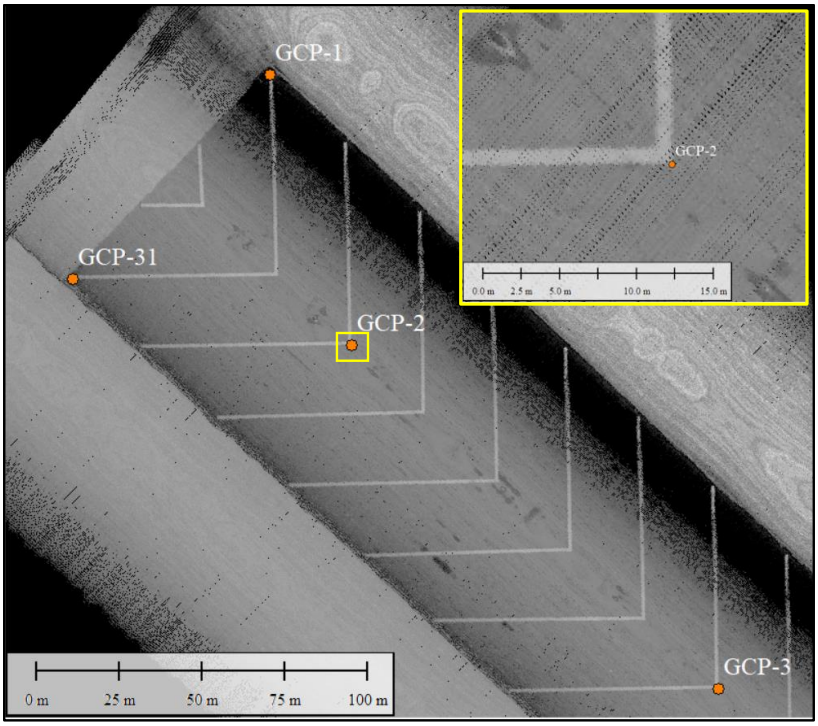

Figure 14: Ground Control Point on the 3D LiDAR Pointcloud

Table 6: mdLiDAR1000 Accuracy Assesment Flights

Date	Number of flights	Base station duration (hh:mm:ss)
27-Oct-17	3	8:52:54
1-Nov-17	5	8:35:11
15-Nov-17	3	7:57:02

2.4 Accuracy Assessment Results

Once the drone landed, the drone data has been processed using mdLiDAR software developed at microdrones and the resulting 3D pointcloud has been used visualized on the runway at Griffiss airport where the control point coordinates have been measured in LP360 environment. Those coordinates have been compared to the land-surveyed ones and the statistics of the differences are listed in Table 7. Those results are the summary of a number of test flights conducted at Griffiss airport.

Table 7: Statistics of Check Point Residuals

	DX (m)	DY (m)	DZ (m)
Minimum	-0.17	-0.11	-0.12
Maximum	0.13	0.14	0.14
Mean	-0.01	0.00	0.01
Sigma	0.06	0.05	0.06
RMS	0.06	0.05	0.06

4. Conclusions

The results presented in the preceding Sections for the mdLiDAR1000 and mdMapper1000DG are interpreted in order to draw the following conclusions,

- Using 2, 3, or 4 strips of image blocks using the mdMapper1000DG system always lead to an accurate image georeferencing resulting in ground object positioning accuracy of about 2-3 pixels in horizontal and about 4-5 pixels in height absolute accuracy when independently evaluated using Check Points.
- 2-strip blocks resulted in a repeatable accuracy of better than 5 cm in both horizontal and height components of ground objects at the 60 m AGL (8 mm GSD) when using the mdMapper1000DG. This confirms that using GNSS/Inertial in conjunction with airborne imagery successfully allows for accurate mapping for ***corridor mapping*** applications. This is a clear differentiator between Direct Georeferencing and the traditional Aerotriangulation or Shape from Motion
- Overlap and sidelap of 80x80 and 80x40 resulted in the same accuracy within the measurement noise level. This confirms repeatable and consistent accuracy amongst different image block configurations.

- The mdLiDA1000 system testing over an accurate set of 56 GCP's resulted in repeatedly a 5 to 6 cm final absolute ground object positioning accuracy when assessing the 3D pointcloud.

5. Acknowledgements

This project has been a collaborative effort of multiple individuals including Jaume C. Mila, and Ivan E. Estruch of Navmatica Corporation, Joe Hutton, and Omer Mien of Applanix Corporation, and Mike Hogan and his team at Microdrones.

6. References

Casella, V., K. Jacobsen, M.M.R. Mostafa, and M. Franzini, 2006. A European Project on Direct Georeferencing, Proceedings, ASPRS Annual conference, Reno, Nevada, May 1-5, 2006

Farrell, J.A. and M. Barth, *The Global Positioning System and Inertial Navigation*, McGraw-Hill, New York, 1999.

Fraser, C.S. 1997. Digital camera self calibration. *ISPRS Journal of Photogrammetry and Remote Sensing* 52(4), 149-159.

Ip, A., N. El-Sheimy, and M.M.R. Mostafa, 2007. Performance Analysis of Integrated Sensor Orientation. *PE&RS*, 73 (1): 89 – 97.

Mostafa, M.M.R. and K.P. Schwarz, 2000. A Multi-Sensor System for Airborne Image Capture and Georeferencing. *PE&RS*, 66 (12): 1417-1424.

Mostafa, M.M.R. and K.P. Schwarz 2001. Digital Image Georeferencing from a Multiple Camera System by GPS/INS. *ISPRS Journal of Photogrammetry and Remote Sensing* 56(1), 1-12.

Mostafa, M.M.R., 2001. Boresight Calibration without Ground Control, Proceedings of OEEPE Workshop: Integrated Sensor Orientation, Hanover, Germany, September 17-18, 2001.

Mostafa, M.M.R., 2001. Boresight Calibration of Integrated Inertial/Camera Systems. Proceedings of the International Symposium on Kinematic Systems in Geodesy, Geomatics and Navigation, Banff, Canada, June 5-8.

Mostafa, M.M.R., 2003. Using Integrated GPS/Inertial Data to Directly Georeference Digital UAV Payload Data, Proceedings UAV Workshop – VITO, Belgium, March 17-18.

Mostafa, M.M.R., 2003. High Precision GPS for Aerial Surveys, Proceedings, The ASPRS Annual Meeting Anchorage, Alaska, USA, May 5-9.

Mostafa, M.M.R., 2004. Airborne GPS Positioning Using Continuously Operating Reference Stations For Mapping Applications. Proceedings of the 4th International Symposium on Mobile Mapping Technology (MMT2004), Kuming, China, March 29-31.

Mostafa, M.M.R., and J. Hutton, 2004. A Fully Integrated Solution for Aerial Surveys: Design, Development, and Performance Analysis, *PE&RS*, 71 (4): 391-399.

Mostafa, M.M.R., 2005. Optimizing the Digital Processing Workflow Using Direct Georeferencing. Proceedings FIG Working Week 2005 and GSDI 8, Cairo, Egypt, 16-21 April, 2005.

Mostafa, M.M.R., E. Roy and X. Zhang, 2007. SmartBase^{TM} — An Efficient New Tool for Aircraft Positioning using Continuously Operated Reference Stations for Mapping Applications. Proceedings, the ASPRS Annual Fall Conference, Ottawa. Canada, October 28 – November 1, 2007.

Mostafa, M.M.R., 2013. Calibration in Multi-Sensor System Environment. Optech Imaging and LiDAR Solutions Conference, held in Toronto, Canada, June 25-27, 2013.

Schwarz, K.P., M.A. Chapman, M.E. Cannon, and P. Gong, 1993. An Integrated INS/GPS Approach to the Georeferencing of Remotely Sensed Data, *PE& RS*, 59(11): 1167-1674.